PCCP

Accepted Manuscript

ROYAL SOCIETY OF CHEMISTRY

www.rsc.org/pccp

Electrophoresis of pH-Regulated Nanoparticles: Impact of Stern Layer

Lanju Mei,[1,+] Tzung-Han Chou,[2,+] Yu-Shen Cheng,[2,+] Ming-Jiang Huang,[2] Li-Hsien Yeh,[2,*] and Shizhi Qian[1,*]

[1]Institute of Micro/Nanotechnology, Old Dominion University, Norfolk, VA 23529, USA

[2]Department of Chemical and Materials Engineering, National Yunlin University of Science and Technology, Yunlin 64002, Taiwan

+ These authors contributed equally to this work

* Corresponding authors:

Fax: +886-5-5312071; E-mail: lhyeh@yuntech.edu.tw (Li-Hsien Yeh)

sqian@odu.edu (Shizhi Qian)

Abstract

A multi-ion model taking into account the Stern layer effect and the surface chemistry reactions is developed for the first time to investigate the surface charge properties and electrophoresis of pH-Regulated silica nanoparticles (NPs). The applicability of the model is validated by comparing its prediction to the experimental data of the electrophoretic mobility of silica NPs available from the literature. Results show that if the particle size is fixed, the Stern layer effect on the surface charge properties of the NP is notable at high pH and background salt concentration; however, that effect on the particle mobility is significant when pH is around neutrality and the slat concentration is medium high (ca. 0.07 M) because of the double-layer polarization effect. Moreover, if pH and the background salt concentration are fixed, the Stern layer effect on the zeta potential and electrophoretic mobility of the NP becomes more significant for smaller particle size. Neglecting the Stern layer effect could result in the overestimation of the zeta potential, surface charge density, and electrophoretic mobility of a NP on the order of several times.

Keywords: Electrokinetics; Zeta Potential; Charge Regulation; Double-Layer Polarization; Stern Layer Capacitance

1. Introduction

Electrophoresis has been widely utilized in diverse fields such as bioanalytical tools,[1, 2] (bio)particle separation,[3, 4] DNA sequencing,[5, 6] and nanoparticle sensing,[7-10] to name a few. Recent progress in nanotechnology enables the use of charge-regulated nanoparticles (NPs) made of, for example, silica,[11-14] Fe_3O_4,[15, 16] and lipids[17] for versatile applications. For example, silica NPs have attracted noteworthy attention of researchers in various fields due to their widespread and potential applications in areas ranging from bioanalytical to biomedical sciences.[11-14] Many researches demonstrated that the stability and the electrophoretic behavior of silica NPs in aqueous solution are highly related to their surface charge properties (e.g., zeta potential and surface charge density),[18-20] which vary with the solution pH and slat concentration. This implies that the charged condition of the surface of silica NPs reveals a charge regulation nature. Therefore, a correct analysis and a fundamental understanding of the surface charge properties of such particles in various solution conditions (e.g., background pH and salt concentration) are crucial for the use of silica NPs in relevant applications.

It is known that a metal oxide surface in contact with an aqueous solution is charged with variations of pH and background salt concentration due to the interfacial chemistry reactions of dissociable functional groups on its wall. Meanwhile, the electrical double layer (EDL), including an immobile Stern layer and a diffusive layer, adjacent to the metal oxide surface is formed. As schematically shown in Fig. 1, the formation of Stern layer by the attraction of compacted counterions on a charged particle surface causes a decrease in the electric potential at the metal-oxide-wall/liquid interface, the so-called surface potential ψ_s, to a lower level called the zeta potential ψ_d (or called electrokinetic potential).[21] Recently, some researches have demonstrated that the Stern layer has a significant influence on the electroosmotic flow,[22] streaming current,[23-26] and ionic conductance[27-30] in a nanochannel or

nanopore. Carrique et al.[31] also studied the Stern layer effect on the electrophoretic motion of the concentrated suspension of colloidal particles without considering the charge regulation nature and the double-layer polarization (DLP) effect stemming from the convective motion of multiple ionic species. They all concluded that the attraction of stagnant counterions within the Stern layer remarkably affects the apparent zeta potential of the nanochannel (or colloid particle). Therefore, the transport phenomena in the nanochannel and the electrophoretic mobility of the suspension of colloidal particle are influenced accordingly. However, to the best of our knowledge, there are still no references to explore the influence of the Stern layer on the electrophoresis of charge-regulated colloidal particles. In previous studies on the surface charge properties[32-34] and the electrophoretic behavior[19, 20, 35-43] of charge-regulated particles, the Stern layer effect was generally neglected, implying that the surface potential at the particle wall/liquid interface and the zeta potential at the Stern layer/diffusive layer interface of charged particles are identical. The assumption of neglecting the Stern layer effect, though makes the analysis much simplifier, could result in not only a wrong estimation of the zeta potential and electrophoretic mobility of particles, but an incorrect description of their behaviors.

In this study, we investigate, for the first time, the surface charge properties and electrophoresis of pH-regulated silica NPs with simultaneous consideration of the Stern layer effect and surface protonation/deprotonation reactions on the particle wall. The model extends the previous analyses, where either the Stern layer effect or the surface chemistry reactions on the particle surface was neglected,[19-21, 31-43] to the more general case much closer to the reality. In addition to the model validation by the existing experimental data of the electrophoretic mobility of silica NPs, the key parameters including the background salt concentration, pH, particle size, and surface capacitance of the Stern layer are examined comprehensively to demonstrate their influences on the zeta potential and electrophoretic

behavior of the silica NP.

2. Theoretical Model

We consider the electrophoresis of a spherical silica NP of radius R_p, driven by an applied uniform electric field, $\mathbf{E}$, of strength E in an incompressible, aqueous Newtonian salt solution containing N types of ionic species, as shown in Fig. 1. The spherical coordinate system (r, θ, φ) with the origin at the center of the NP is adopted, and $\mathbf{E}$ is applied in the $z-$direction (parallel to $\theta = 0$).

2.1 Charge regulation and basic Stern layer model

Due to the interfacial chemistry reactions of plentiful silanol ($\mathrm{Si-OH}$) functional groups, the silica NPs in contact with an aqueous solution bear surface charges. Suppose that the silanol groups undergo the following two interfacial deprotonation and protonation reactions, $\mathrm{Si-OH} \leftrightarrow \mathrm{Si-O^- + H^+}$ and $\mathrm{Si-OH + H^+} \leftrightarrow \mathrm{Si-OH_2^+}$, respectively. Let K_A and K_B be the equilibrium constants of the above two reactions, respectively. The surface charge density of the silica NP, σ_s, can be expressed as

$$\sigma_s = -\left(\frac{FN_{total}\times 10^{18}}{N_a}\right)\left\{\frac{10^{-\mathrm{p}K_A} - 10^{-\mathrm{p}K_B}\left[\mathrm{H^+}\right]_s^2}{10^{-\mathrm{p}K_A} + \left[\mathrm{H^+}\right]_s + 10^{-\mathrm{p}K_B}\left[\mathrm{H^+}\right]_s^2}\right\}. \quad (1)$$

Here, $\mathrm{p}K_j = -\log K_j$, $j = A$ and B; N_{total} (in the unit of sites/nm^2) is the total number site density of functional groups on the NP surface; N_a and F are the Avogadro's number and Faraday constant, respectively; $[\mathrm{H^+}]_s$ is the surface concentration of protons on the NP. If the particle-particle interaction is neglected, $[\mathrm{H^+}]_s$ can be described by the Boltzmann distribution, that is,

$$[\mathrm{H^+}]_s = 10^{-\mathrm{pH}}\exp\left(-\frac{F\psi_s}{RT}\right), \quad (2)$$

where R and T are the universal gas constant and absolute temperature, respectively; ψ_s

is the surface potential of the NP.

Equations (1) and (2) imply that σ_s is dominated by ψ_s (not the zeta potential of the NP, ψ_d), but in previous literatures for charge-regulated particles,[19, 20, 32-48] ψ_s is all assumed to be the same as ψ_d for simplicity. Note that only ψ_d (not ψ_s) can be determined directly from experimental measurements. This is because when a charged particle is immersed in an aqueous salt concentration, the EDL, including a Stern layer and a diffusive layer, forms immediately, and the attraction of compacted counterions in the Stern layer results in a significant decrease in ψ_s to a lower level called ψ_d, as shown in Fig. 1. Suppose that counterions inside the Stern layer are immobile.[49] The electric potential (ϕ) within that layer can be described by

$$\frac{1}{r^2}\frac{d}{dr}\left(r^2\frac{d\phi}{dr}\right)=0 \quad (R_p \le r \le R_p + h_s), \tag{3}$$

where h_s is the thickness of the Stern layer, which is very thin (i.e. 1-3 times ionic size) compared to the NP radius and can be neglected ($h_s \to 0$). Solving eqn (3) subject to the boundary conditions, (i) $\phi = \psi_s$ at $r = R_p$ and (ii) $\phi = \psi_d$ at $r = R_p + h_s$, yields

$$\phi = \frac{\left(\frac{1}{R_p}-\frac{1}{r}\right)}{\left(\frac{1}{R_p}-\frac{1}{R_p+h_s}\right)}\left(\psi_d-\psi_s\right)+\psi_s . \tag{4}$$

Consequently, the relationship between ψ_s and ψ_d can be described by the following basic Stern layer model,

$$\sigma_s = -\varepsilon_f \mathbf{n}\cdot\nabla\phi\big|_{r=R_p} = -\varepsilon_f \left.\frac{d\phi}{dr}\right|_{r=R_p} = \varepsilon_f\left(\frac{1}{h_s}+\frac{1}{R_p}\right)\left(\psi_s-\psi_d\right) = C_s\left(\psi_s-\psi_d\right), \tag{5}$$

where ε_f is the permittivity of the liquid phase, **n** is the unit normal vector directed into the

fluid phase, and $C_s = \varepsilon_f \left(\frac{1}{h_s} + \frac{1}{R_p} \right) \approx \varepsilon_f / h_s$ is the surface capacitance of the Stern layer on the NP.[50]

2.2 Governing equations and boundary conditions for electrophoretic motion of NP

Suppose that the strength of $\mathbf{E}$ is much weaker than that of equilibrium electric field established by the charged silica NP.[51] Similar to the treatments of O'Brien and White,[52] and Ohshima,[53] the present problem can be solved by the perturbation approach, where a dependent variable can be decomposed into an equilibrium term and a perturbed term, denoted by a subscript e and a prefix δ, respectively,[51] representing the value of that variable in the absence and presence of external electric field $\mathbf{E}$, respectively. For example, the electric potential (ψ) within the liquid phase ($r \geq R_p + h_s$) can be expressed as $\psi = \psi_e + \delta\psi$, where ψ_e and $\delta\psi$ are the equilibrium potential and the perturbed potential, respectively. Moreover, we assume that the dispersion is so dilute that the presence of particle-particle interaction is neglected, the system is at a quasi-steady state, and the flow is in the creeping regime. Taking into account the double layer polarization (DLP) effect arising from the convective motion of ionic species around the EDL of a charged NP, it can be shown that the governing equations for the electric, ionic concentration, and flow fields within the liquid phase can be summarized, in scaled forms, as[19, 42]

$$\nabla^{*2} \psi_e^* = -\frac{\left(\kappa R_p\right)^2}{\sum_{i=1}^{N} \frac{z_i^2 c_{i0}}{z_1^2 c_{10}}} \sum_{i=1}^{N} \frac{z_i c_{i0}}{z_1 c_{10}} \exp\left(-\frac{z_i \psi_e^*}{z_1} \right), \tag{6}$$

$$\nabla^{*2} \delta\psi^* = \frac{\left(\kappa R_p\right)^2}{\sum_{i=1}^{N} \frac{z_i^2 c_{i0}}{z_1^2 c_{10}}} \sum_{i=1}^{N} \frac{z_i^2 c_{i0}}{z_1^2 c_{10}} \left(\delta\psi^* + g_i^* \right) \exp\left(-\frac{z_i \psi_e^*}{z_1} \right), \tag{7}$$

$$\nabla^{*2} g_i^* - \frac{z_i}{z_1} \nabla^* \psi_e^* \cdot \nabla^* g_i^* - Pe_i \left(\mathbf{u}^* \cdot \nabla^* \psi_e^* \right) = 0, \quad i = 1, 2, \ldots N \tag{8}$$

$$c_i^* = \exp\left(-\frac{z_i \psi_e^*}{z_1}\right)\left[1-\frac{z_i}{z_1}\left(\delta\psi^* + g_i^*\right)\right],\ i = 1,2,\ldots N \tag{9}$$

$$\nabla^{*2}\mathbf{u}^* - \nabla^*\delta p^* + \nabla^{*2}\psi_e^*\nabla^*\delta\psi^* + \nabla^{*2}\delta\psi^*\nabla^*\psi_e^* = \mathbf{0}, \tag{10}$$

$$\nabla^* \cdot \mathbf{u}^* = 0. \tag{11}$$

In the above, $\nabla^* = R_p\nabla$, $\nabla^{*2} = R_p{}^2\nabla^2$, $\psi_e^* = \psi_e/\psi_{ref}$, $\delta\psi^* = \delta\psi/\psi_{ref}$, $g_i^* = g_i/\psi_{ref}$, $c_i^* = c_i/c_{i0}$, $\mathbf{u}^* = \mathbf{u}/U_{ref}$, and $\delta p^* = \delta p/p_{ref}$ with $\psi_{ref} = RT/Fz_1$, $U_{ref} = \varepsilon_f(\psi_{ref})^2/\eta R_p$, and $p_{ref} = \varepsilon_f(\psi_{ref}/R_p)^2$ being the reference thermal potential, velocity, and pressure, respectively. $\kappa = \left[\sum_{i=1}^{N} c_{i0}(Fz_i)^2/\varepsilon_f RT\right]^{1/2}$ is the reciprocal of Debye length; z_i, c_i, D_i, and $Pe_i = \varepsilon_f(\psi_{ref})^2/\eta D_i$ are the valence, concentration, diffusivity, and electric Peclet number of ionic species i, respectively; η is the dynamic viscosity of the liquid phase; g_i is a hypothetical perturbed potential describing a polarized EDL; $\mathbf{u}$ is the fluid velocity relative to the particle; δp is the external pressure; c_{i0} is the bulk concentration of ionic species i far away from the charged particle. Note that c_i and c_{i0} are all in the SI unit of mM in the present study.

The following boundary conditions are specified for eqn (7)-(11): (i) At a point far away from the particle, the electric, ionic concentration, and flow fields are not influenced by its presence, implying that $\mathbf{n}\cdot\nabla^*\psi_e^* = 0$, $\mathbf{n}\cdot\nabla^*\delta\psi^* = -E^*\cos\theta$, $g_i^* = -\delta\psi^*$, and $\mathbf{u}^* = -U_p^*\mathbf{e}_z$,[54] where $E^* = E/E_{ref}$, $U_p^* = U_p/U_{ref}$, $E_{ref} = \psi_{ref}/R_p$, $\mathbf{e}_z$ is the unit vector in the z direction, and U_p is the electrophoretic velocity of the silica NP. (ii) Because the Stern layer is very thin and ions and fluid inside that layer are stationary, the no-slip, nonconductive, and ion-impenetrable boundary conditions are applied at the Stern layer/liquid interface ($r = R_p + h_s$), yielding $\mathbf{u}^* = 0$, $\mathbf{n}\cdot\nabla^*\delta\psi^* = 0$, and $\mathbf{n}\cdot\nabla g_i^* = 0$, respectively. (iii) Because the

equilibrium electric potential and field are continuous at the Stern layer/liquid interface ($r = R_p + h_s$),[55] $\psi_e = \phi = \psi_d$ and $\mathbf{n}\cdot\nabla\psi_e = \mathbf{n}\cdot\nabla\phi$. If $h_s << R_p$, substituting eqn (4) into $\mathbf{n}\cdot\nabla\psi_e = \mathbf{n}\cdot\nabla\phi$ at $r = R_p + h_s$ yields

$$\mathbf{n}\cdot\nabla\psi_e = \mathbf{n}\cdot\nabla\phi \approx -\frac{C_s\left(\psi_s - \psi_d\right)}{\varepsilon_f}. \tag{12}$$

Combining eqn (1), (5), and (12), we obtain the following boundary condition for ψ_e^* at $r = R_p + h_s$,

$$\mathbf{n}\cdot\nabla^*\psi_e^* = -\frac{\sigma_s}{\varepsilon_f\left(\psi_{ref}/R_p\right)}$$
$$= \left(\frac{FN_{total}R_p\times 10^{18}}{\varepsilon_f N_a \psi_{ref}}\right)\left\{\frac{10^{-\mathrm{p}K_A} - 10^{-\mathrm{p}K_B}\left[10^{-\mathrm{pH}}\exp\left(-\frac{F\psi_s}{RT}\right)\right]^2}{10^{-\mathrm{p}K_A} + \left[10^{-\mathrm{pH}}\exp\left(-\frac{F\psi_s}{RT}\right)\right] + 10^{-\mathrm{p}K_B}\left[10^{-\mathrm{pH}}\exp\left(-\frac{F\psi_s}{RT}\right)\right]^2}\right\}, \tag{13}$$

where ψ_s, based on eqn (12), can be replaced by

$$\psi_s = \left(\psi_e - \frac{\varepsilon_f \mathbf{n}\cdot\nabla\psi_e}{C_s}\right)\Bigg|_{r=R_p+h_s}. \tag{14}$$

2.3 Electrophoretic mobility of the silica NP

The forces acting on the silica NP include an electrical driving force, F_e, and a hydrodynamic drag force, F_h. Assuming that the considered system is in a quasi-steady state, the forces acting on the particle in the *z* direction should vanish, that is, $F_{ez} + F_{hz} = 0$. In this case, F_{ez} and F_{hz} can be evaluated, respectively, by the surface integration of the Maxwell stress tensor, $\boldsymbol{\sigma}^{\mathbf{E}}$, and the hydrodynamic stress tensor, $\boldsymbol{\sigma}^{\mathbf{H}}$, over the Stern layer/liquid interface of the particle, S. It can be shown that[51]

$$F_{ez} = \iint_S \left(\frac{\partial\psi_e}{\partial n}\frac{\partial\delta\psi}{\partial z} - \frac{\partial\psi_e}{\partial t}\frac{\partial\delta\psi}{\partial t}n_z\right)dS, \tag{15}$$

$$F_{hz} = \iint_S \left(\boldsymbol{\sigma}^{\mathbf{H}} \cdot \mathbf{n}\right) \cdot \mathbf{e}_z dS \,, \tag{16}$$

where n_z is the z component of **n**; $\partial / \partial n$ and $\partial / \partial t$ are the rate of variation in the direction of **n** and that of the unit tangential vector **t**, respectively.

To obtain the electrophoretic mobility of the silica NP, $\mu = U_p / E$, a trial-and-error solution procedure needs be applied as the follows. (i) For given conditions along with a given E, an initial value of U_p, which can be estimated by the approach proposed by Hsu and Tai[19] without considering the Stern layer effect, is assumed, and then solve eqn (6)-(11) subject to the boundary conditions assumed. (ii) Calculate F_{ez} and F_{hz} by eqn (15) and (16), respectively. (iii) Check if $\left|F_{ez} + F_{hz}\right| < 10^{-6}$. If it is satisfied, the assumed U_p is correct; otherwise, U_p is adjusted based on the Newton-Raphson method. (iv) The scaled electrophoretic mobility of the silica NP, μ^*, can be obtained by $\mu^* = \mu / \left(U_{ref} / E_{ref}\right)$.

3. Results and Discussion

The present problem is numerically solved by the commercial finite element software, FlexPDE (version 4.24), which was found to be adequately efficient and accurate for solving similar electrokinetic problems without considering the Stern layer effect.[19, 20, 36-42]

3.1 Verification by experimental data

To validate our model with the Stern layer effect, it is first used to fit the experimental data of Sonnefeld et al.,[56] where the electrophoretic mobility of silica NPs of 20 nm in radius as a function of pH in 0.001 M aqueous NaCl solution was performed. To simulate the experimental condition, we assume that there are four major ionic species ($N = 4$), H^+, OH^-, Na^+, and Cl^-, in solution. Let c_{i0} ($i = 1$, 2, 3, and 4) be the bulk concentration of these ions, respectively, and C_{NaCl} (in the unit of M) be the molar concentration of background salt. It can be shown that electroneutrality results in $c_{10} = 10^{-\mathrm{pH}+3}$,

$c_{20} = 10^{-(14-\mathrm{pH})+3}$, $c_{30} = 10^3 \times C_{\mathrm{NaCl}}$, and $c_{40} = 10^3 \times (C_{\mathrm{NaCl}} + 10^{-\mathrm{pH}} - 10^{-(14-\mathrm{pH})})$ when $\mathrm{pH} \le 7$; otherwise, $c_{30} = 10^3 \times (C_{\mathrm{NaCl}} - 10^{-\mathrm{pH}} + 10^{-(14-\mathrm{pH})})$ and $c_{40} = 10^3 \times C_{\mathrm{NaCl}}$ when $\mathrm{pH} > 7$.[57, 58] Fig. 2 shows that the prediction from our model (curve) at $N_{total} = 7$ sites/nm^2, $\mathrm{p}K_A = 6.8$, $\mathrm{p}K_B = 2$, and $C_s = 2.5$ F/m^2 coincides very well with the experimental data (diamonds) in the entire pH region considered. In addition, the fitted parameters are in accordance with the reported values of silica in the literatures (e.g., $N_{total} = 3.8 \sim 8$ sites/nm^2, $\mathrm{p}K_A = 6 \sim 8$, $\mathrm{p}K_B = 0 \sim 3$, and $C_s = 0.15 \sim 2.9$ F/m^2).[27, 29, 59] It is thus confirmed that the present model is capable of capturing the underlying physics of the electrophoresis of silica NPs in the wide range of the solution pH.

In subsequent sections, the verified model along with the above fitted parameters of C_s, N_{total}, $\mathrm{p}K_A$, and $\mathrm{p}K_B$ is then used to further investigate the effect of the Stern layer on the surface charge properties and the electrophoretic motion of a silica NP as functions of pH and background salt concentration of NaCl. Unless otherwise specified, the radius of a silica NP is fixed at $R_p = 15$ nm.

3.2 Stern layer effect on surface charge properties of a silica NP

Fig. 3 and 4 depict the Stern layer effect on the variations of the zeta potential, ψ_d, and surface charge density, σ_s, with pH and the background salt concentration C_{NaCl}; both the calculated results from the models with (curves) and without (spheres) considering the Stern layer effect are presented. In these two figures, the larger the value of the surface capacitance of the Stern layer C_s represents the less significant the Stern layer effect, implying that the Stern layer effect can be neglected as $C_s \to \infty$ (solid curve) and, therefore, $\psi_d = \psi_s$, which is the typical assumption made in previous electrokinetic studies ignoring the Stern layer effect.[19, 20, 32-48] As shown in Fig. 3 and 4, the results obtained from the present model at

$C_s \to \infty$ (solid curve) match consistently with those from the previous model without considering the Stern layer effect (spheres), proving the soundness of the present model.

It is worth noting in Fig. 3 and 4 that the Stern layer effect on the surface charge properties (ψ_d and σ_s) of a silica NP is significant when the background pH and salt concentration C_{NaCl} are high. That is, the larger the values of pH and C_{NaCl}, the more remarkable deviation of ψ_d and σ_s for C_s decreasing from an infinite value to 0.15. The more significant Stern layer effect on ψ_d and σ_s for higher pH arises from the fact that the surface charges of a silica NP increases as pH increases due to a greater number of the negatively charged functional groups ($\mathrm{SiO^-}$) dissociated from silanol groups, attracting more counterions near the particle surface. This results in a more significant difference between ψ_d and ψ_s, and therefore the Stern layer effect. Similarly, an increase in C_{NaCl} results in a decrease in the EDL thickness, leading to more counterions confined on the NP surface and also more remarkable Stern layer effect. Fig. 3 and 4 suggest that neglecting the Stern layer effect could result in an overestimation of ψ_d (σ_s) between $C_s = 0.15\ \mathrm{F/m^2}$ and $C_s \to \infty$, calculated by $\left|\psi_d\left(C_s = 0.15\ \mathrm{F/m^2}\right) - \psi_d\left(C_s \to \infty\right)\right| / \psi_d\left(C_s = 0.15\ \mathrm{F/m^2}\right) \times 100\%$ ($\left|\sigma_s\left(C_s = 0.15\ \mathrm{F/m^2}\right) - \sigma_s\left(C_s \to \infty\right)\right| / \sigma_s\left(C_s = 0.15\ \mathrm{F/m^2}\right) \times 100\%$), are up as high as 454 % (702 %) at pH=8 and $C_{\mathrm{NaCl}} = 0.1$ M. This implies that neglect of the Stern layer effect, which was assumed in previous studies,[19, 20, 32-48] might cause an apparently wrong estimation of the surface charge properties of a silica NP.

3.3 Stern layer effect on electrophoretic motion of a silica NP

Fig. 5 and 6 depict the Stern layer effect on the scaled electrophoretic mobility, μ^*, of a silica NP as a function of pH and the background salt concentration C_{NaCl}. These two figures reveal that the dependence of the electrophoretic behavior of a silica NP on pH and C_{NaCl}

depends significantly on the value of the surface capacitance of the Stern layer C_s. For example, if the Stern layer effect is neglected (e.g., $C_s \to \infty$) and extremely significant (e.g., $C_s = 0.15$ F/m^2), $|\mu^*|$ increases monotonically with increasing pH; however, if the Stern layer effect is moderate (e.g., $C_s = 0.6$ and 2.4 F/m^2), $|\mu^*|$ first increases with an increase in pH and then shows a local maximum as pH further increases to a sufficiently large value, as shown in Fig. 5. Note that the magnitude of the zeta potential (ψ_d) of a silica NP increases with an increase in pH and C_s, as shown in Fig. 3a, resulting in an increase in its electrical driving force and electrophoretic mobility. However, an apparent increase in $|\psi_d|$ meanwhile leads to a more significant DLP effect,[60, 61] which establishes a polarized local electric field in the opposite direction of the applied one and, therefore, lowers the particle mobility. Consequently, if μ^* is dominated by the effect of increasing $|\psi_d|$ with increasing pH, $|\mu^*|$ increases accordingly; however, if μ^* is dominated by the effect of DLP, $|\mu^*|$ decreases with an increase in pH at sufficiently high pH. Note that if pH is sufficiently high and deviates appreciably from 7, the ionic strength of solution becomes higher. This yields a thinner EDL and also reduces the particle mobility.

Fig. 6 reveals that if the Stern layer effect is very significant (e.g., $C_s = 0.15$ F/m^2), $|\mu^*|$ decreases with increasing C_{NaCl}, which is expected because the electrical driving force decreases as C_{NaCl} increases. On the other hand, if the Stern layer effect becomes relatively insignificant, $|\mu^*|$ shows both a local minimum and a local maximum as C_{NaCl} increases. This can be attributed to the significant DLP effect, which is remarkable when the EDL thickness becomes comparable to the particle size, typically occurring at $1 \le \kappa R_p \le 4$,[61] and the zeta potential of a particle is extremely high at sufficiently large C_s. The significant DLP

effect causes an appreciable decrease in the electrical driving force and, therefore, a remarkable local minimum of the particle mobility at medium C_{NaCl}, as show in Fig. 6.

It is worth noting in Fig. 5 and 6 that the Stern layer effect on the electrophoretic mobility of a silica NP is significant when pH is around neutrality and C_{NaCl} is medium high, which is apparently inconsistent with the results of its surface charge properties shown in Fig. 3 and 4, in which the Stern layer effect on ψ_d and σ_s is significant with increasing pH and C_{NaCl}. For example, the maximum relative difference of μ^* between the results at $C_s = 0.15$ F/m^2 and $C_s \to \infty$, calculated by $\left|\mu^*\left(\text{dash-dotted curve}\right) - \mu^*\left(\text{solid curve}\right)\right| / \mu^*\left(\text{dash-dotted curve}\right) \times 100\%$, is ca. 40.8 % at pH 6 for a fixed $C_{\mathrm{NaCl}} = 0.001$ M (Fig. 5) and 191 % at $C_{\mathrm{NaCl}} = 0.07$ M for a fixed pH 8 (Fig. 6). This can be attributed to the aforementioned DLP effect, which reduces the particle mobility and becomes significant when the surface charge of a silica NP is large (high pH) and the NP's size is comparable to the EDL thickness (moderate κR_p). Consequently, the relative deviation of μ^* between the results with and without considering the Stern layer effect no longer gets remarkable with continuously increasing pH and C_{NaCl}.

3.4 Influence of particle size

Fig. 7 depicts the influences of the particle size, $D_p = 2R_p$, and the surface capacitance of the Stern layer C_s on the surface potential ψ_s, zeta potential ψ_d, and scaled electrophoretic mobility μ^* of a silica NP. As shown in Fig. 7a, the magnitude of ψ_d (dashed curves) increases, while that of ψ_s (solid curves) decreases with increasing C_s. If C_s is sufficiently large, the value of ψ_d is close to that of ψ_s. These behaviors are expected since the larger the value of C_s, the less significant the Stern layer effect and,

therefore, the smaller the difference between ψ_d and ψ_s. Fig. 7a also indicates that the magnitude of ψ_d and ψ_s increases with an increase in D_p. This can be attributed to an increase in the surface charges of a silica NP with increasing D_p due to an increase in its surface area.

Fig. 7b shows that if the particle size is sufficiently small (e.g., $D_p = 10$ nm), $|\mu^*|$ decreases monotonically with increasing C_s. Note that in this case, $\kappa R_p = 0.52$ under the considered solution property, implying that the DLP effect is relatively insignificant. Therefore, the behavior of μ^* is dominated primarily by the increase of $|\psi_d|$ with increasing C_s. On the other hand, if the particle size is large (e.g., $D_p = 30$ and 60 nm), $|\mu^*|$ first decreases with increasing C_s when C_s is small and then goes through a local minimum when C_s is sufficiently large. This can be explained by the fact that the DLP effect on these two sizes of silica NP becomes extremely significant ($\kappa R_p = 1.55$ and 3.09 for $D_p = 30$ and 60 nm, respectively) when C_s is sufficiently large due to their apparently large zeta potential shown in Fig. 7a. Note that under the considered solution properties, Fig. 7 also indicates that the smaller the particle size the more apparent relative deviation of ψ_d and μ^* between the cases for $C_s = 0.1$ and 30 F/m^2, implying that the Stern layer effect on the zeta potential and electrophoretic mobility of a silica NP becomes more significant for smaller particle size.

4. Conclusions

The Stern layer effect on the surface charge properties and electrophoresis of silica nanoparticles (NPs) is investigated for the first time with simultaneous consideration of interfacial chemical reactions on the particle wall and multiple ionic species. The model developed is validated by the existing experimental data of the electrophoretic mobility of

silica NPs. Results show that if the particle size is fixed, the Stern layer effect on the zeta potential and surface charge density of the silica NP is more significant for higher pH and background salt concentration, while that effect on its mobility is remarkable when pH is around neutrality and the salt concentration is medium high. If the solution properties are fixed, the Stern layer effect on both the zeta potential and electrophoretic mobility of the silica NP is more profound for relatively small particle size. In addition to its quantitative value, the qualitative behavior of the particle mobility as functions of pH and background salt concentration depends apparently on how significant the Stern layer effect is. Neglecting the Stern layer effect could cause not only the overestimation of the zeta potential, surface charge density, and electrophoretic mobility of the silica NP on the order of several times but also an incorrect estimation of the relevant electrophoretic behaviors under certain conditions.

Acknowledgements

This work is supported by the Ministry of Science and Technology of the Republic of China under Grants MOST 102-2221-E-224-052-MY3, 103-2221-E-224-039-MY3 (L.H.Y.), and 103-2221-E-224-077-MY2 (T.H.C.), and the China Scholarship Council (L.M.).

References

1. A. Pallandre, B. de Lambert, R. Attia, A. M. Jonas and J. L. Viovy, *Electrophoresis*, 2006, **27**, 584-610.

2. J. H. Guo, X. W. Huang and Y. Ai, *Anal. Chem.*, 2015, **87**, 6516-6519.

3. X. C. Xuan, J. J. Zhu and C. Church, *Microfluid. Nanofluid.*, 2010, **9**, 1-16.

4. J. S. Mellors, K. Jorabchi, L. M. Smith and J. M. Ramsey, *Anal. Chem.*, 2010, **82**, 967-973.

5. C. Dekker, *Nat. Nanotechnol.*, 2007, **2**, 209-215.

6. B. M. Venkatesan and R. Bashir, *Nat. Nanotechnol.*, 2011, **6**, 615-624.

7. L. H. Yeh, M. K. Zhang, S. W. Joo, S. Qian and J. P. Hsu, *Anal. Chem.*, 2012, **84**, 9615-9622.

8. S. R. German, L. Luo, H. S. White and T. L. Mega, *J. Phys. Chem. C*, 2013, **117**, 703-711.

9. H. W. Wu, H. Liu, S. W. Tan, J. J. Yu, W. Y. Zhao, L. Wang and Q. J. Liu, *J. Phys. Chem. C*, 2014, **118**, 26825-26835.

10. W. J. Lan, C. Kubeil, J. W. Xiong, A. Bund and H. S. White, *J. Phys. Chem. C*, 2014, **118**, 2726-2734.

11. T. Yu, A. Malugin and H. Ghandehari, *ACS Nano*, 2011, **5**, 5717-5728.

12. S. V. Patwardhan, F. S. Emami, R. J. Berry, S. E. Jones, R. R. Naik, O. Deschaume, H. Heinz and C. C. Perry, *J. Am. Chem. Soc.*, 2012, **134**, 6244-6256.

13. A. Lesniak, F. Fenaroli, M. R. Monopoli, C. Aberg, K. A. Dawson and A. Salvati, *ACS Nano*, 2012, **6**, 5845-5857.

14. D. Tarn, C. E. Ashley, M. Xue, E. C. Carnes, J. I. Zink and C. J. Brinker, *Accounts Chem. Res.*, 2013, **46**, 792-801.

15. A. Mitra, J. Mohapatra, S. S. Meena, C. V. Tomy and M. Aslam, *J. Phys. Chem. C*, 2014, **118**, 19356-19362.

16. A. Lak, M. Kraken, F. Ludwig, A. Kornowski, D. Eberbeck, S. Sievers, F. J. Litterst, H.

Weller and M. Schilling, *Nanoscale*, 2013, **5**, 12286-12295.

17. S. W. Tan, X. Li, Y. J. Guo and Z. P. Zhang, *Nanoscale*, 2013, **5**, 860-872.
18. M. L. Fisher, M. Colic, M. P. Rao and F. F. Lange, *J. Am. Ceram. Soc.*, 2001, **84**, 713-718.
19. J. P. Hsu and Y. H. Tai, *Langmuir*, 2010, **26**, 16857-16864.
20. C. Hsu, D. J. Lee, J. P. Hsu, N. Wang and S. Tseng, *AIChE J.*, 2014, **60**, 451-458.
21. J. Lyklema and J. T. G. Overbeek, *J. Colloid Interface Sci.*, 1961, **16**, 501-512.
22. C. Hughes, L. H. Yeh and S. Qian, *J. Phys. Chem. C*, 2013, **117**, 9322-9331.
23. F. H. J. van der Heyden, D. J. Bonthuis, D. Stein, C. Meyer and C. Dekker, *Nano Lett.*, 2007, **7**, 1022-1025.
24. S. Xue, L. H. Yeh, Y. Ma and S. Z. Qian, *J. Phys. Chem. C*, 2014, **118**, 6090-6099.
25. L. H. Yeh, Y. Ma, S. Xue and S. Qian, *Electrochem. Commun.*, 2014, **48**, 77-80.
26. C. Davidson and X. C. Xuan, *Electrophoresis*, 2008, **29**, 1125-1130.
27. M. B. Andersen, J. Frey, S. Pennathur and H. Bruus, *J. Colloid Interface Sci.*, 2011, **353**, 301-310.
28. Y. Ma, S. Xue, S. C. Hsu, L. H. Yeh, S. Qian and H. Tan, *Phys. Chem. Chem. Phys.*, 2014, **16**, 20138-20146.
29. Y. Ma, L. H. Yeh, C. Y. Lin, L. J. Mei and S. Z. Qian, *Anal. Chem.*, 2015, **87**, 4508-4514.
30. L. H. Yeh, Y. Ma, S. Xue and S. Z. Qian, *Sens. Actuator B-Chem.*, 2015, **215**, 266-271.
31. F. Carrique, F. J. Arroyo and A. V. Delgado, *J. Colloid Interface Sci.*, 2001, **243**, 351-361.
32. M. Barisik, S. Atalay, A. Beskok and S. Z. Qian, *J. Phys. Chem. C*, 2014, **118**, 1836-1842.
33. S. Atalay, Y. Ma and S. Qian, *J. Colloid Interface Sci.*, 2014, **425**, 128-130.
34. S. Atalay, M. Barisik, A. Beskok and S. Z. Qian, *J. Phys. Chem. C*, 2014, **118**,

10927-10935.

35. H. J. Keh and J. M. Ding, *Langmuir*, 2002, **18**, 4572-4583.

36. J. P. Hsu, Y. H. Tai, L. H. Yeh and S. Tseng, *J. Phys. Chem. B*, 2011, **115**, 3972-3980.

37. J. P. Hsu, Y. H. Tai, L. H. Yeh and S. J. Tseng, *Langmuir*, 2012, **28**, 1013-1019.

38. J. P. Hsu, C. P. Yee and L. H. Yeh, *Langmuir*, 2012, **28**, 10942-10947.

39. J. P. Hsu, C. H. Huang and S. Tseng, *Electrophoresis*, 2013, **34**, 785-791.

40. J. P. Hsu, C. H. Huang and S. Tseng, *Soft Matter*, 2013, **9**, 11534-11541.

41. N. Wang, C. P. Yee, Y. Y. Chen, J. P. Hsu and S. Tseng, *Langmuir*, 2013, **29**, 7162-7169.

42. C. Hsu, T. W. Lo, D. J. Lee and J. P. Hsu, *Langmuir*, 2013, **29**, 2427-2433.

43. Y. Y. Chen, J. P. Hsu and S. Tseng, *J. Colloid Interface Sci.*, 2014, **421**, 154-159.

44. H. J. Keh and Y. L. Li, *Langmuir*, 2007, **23**, 1061-1072.

45. J. Lou, C. Y. Shih and E. Lee, *Langmuir*, 2010, **26**, 47-55.

46. J. P. Hsu, W. L. Hsu and K. L. Liu, *Langmuir*, 2010, **26**, 8648-8658.

47. J. P. Hsu and Y. K. Fu, *J. Phys. Chem. C*, 2012, **116**, 15126-15133.

48. S. Tseng, T. W. Lo, C. Hsu, Y. K. Fu and J. P. Hsu, *Phys. Chem. Chem. Phys.*, 2013, **15**, 7512-7519.

49. Y. Ma, L. H. Yeh, S. Qian, J. P. Hsu and S. Tseng, *Electrochem. Commun.*, 2014, **45**, 75-78.

50. S. H. Behrens and D. G. Grier, *J. Chem. Phys.*, 2001, **115**, 6716-6721.

51. J. P. Hsu, L. H. Yeh and M. H. Ku, *J. Colloid Interface Sci.*, 2007, **305**, 324-329.

52. R. W. O'brien and L. R. White, *J. Chem. Soc. Faraday Trans. 2*, 1978, **74**, 1607-1626.

53. H. Ohshima, *Adv. Colloid Interface Sci.*, 1995, **62**, 189-235.

54. L. H. Yeh, Y. H. Tai, N. Wang, J. P. Hsu and S. Qian, *Nanoscale*, 2012, **4**, 7575-7584.

55. M. J. Huang, L. J. Mei, L. H. Yeh and S. Z. Qian, *Electrochem. Commun.*, 2015, **55**, 60-63.

56. J. Sonnefeld, M. Lobbus and W. Vogelsberger, *Colloid Surf. A-Physicochem. Eng. Asp.*, 2001, **195**, 215-225.

57. L. H. Yeh, M. Zhang and S. Qian, *Anal. Chem.*, 2013, **85**, 7527-7534.

58. Y. Ma, L. H. Yeh and S. Qian, *Electrochem. Commun.*, 2014, **43**, 91-94.

59. F. H. J. van der Heyden, D. Stein and C. Dekker, *Phys. Rev. Lett.*, 2005, **95**, 116104.

60. L. H. Yeh and J. P. Hsu, *Soft Matter*, 2011, **7**, 396-411.

61. L. H. Yeh, K. L. Liu and J. P. Hsu, *J. Phys. Chem. C*, 2012, **116**, 367-373.

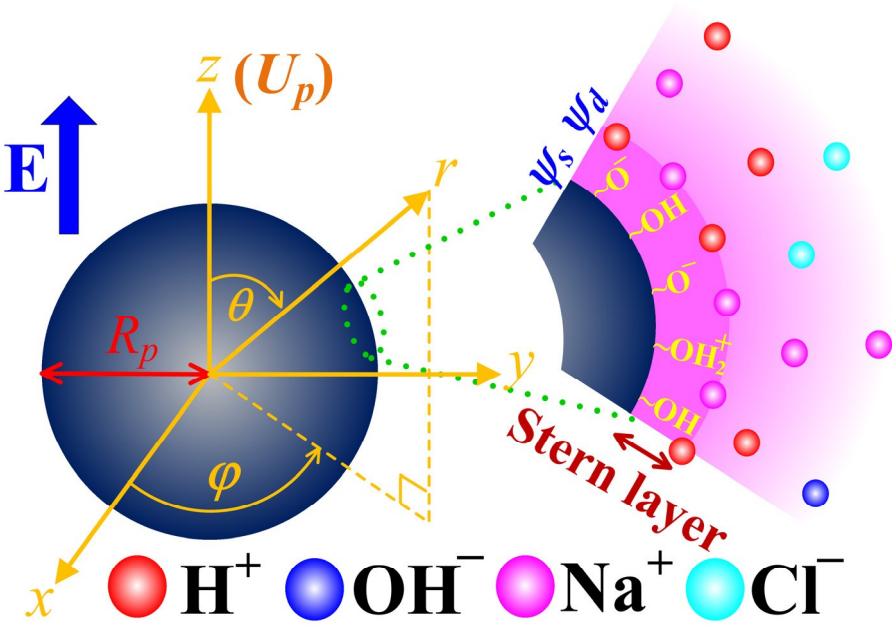

Fig. 1. Schematic of the system under consideration where a charge-regulated silica NP of radius R_p immersed in a general salt solution containing multiple ionic species, H^+, OH^-, Na^+, and Cl^-, is electrophoretically driven by a uniformly applied electric field $\mathbf{E}$ in the $z-$direction (not to scale). ψ_s and ψ_d are the surface and zeta potentials of the charged silica NP, respectively.

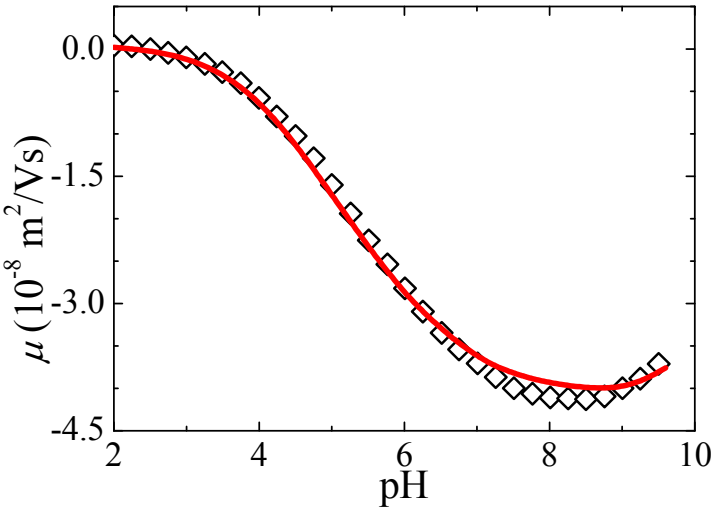

Fig. 2. Dependence of the electrophoretic mobility μ on the solution pH for the case of silica nanoparticles of radius 20 nm in 0.001 M NaCl solution. Diamonds: experimental data of Sonnefeld et al.[56]; curve: present results at $N_{total} = 7$ sites/nm^2, $\mathrm{p}K_A = 6.8$, $\mathrm{p}K_B = 2$, and $C_s = 2.5$ F/m^2.

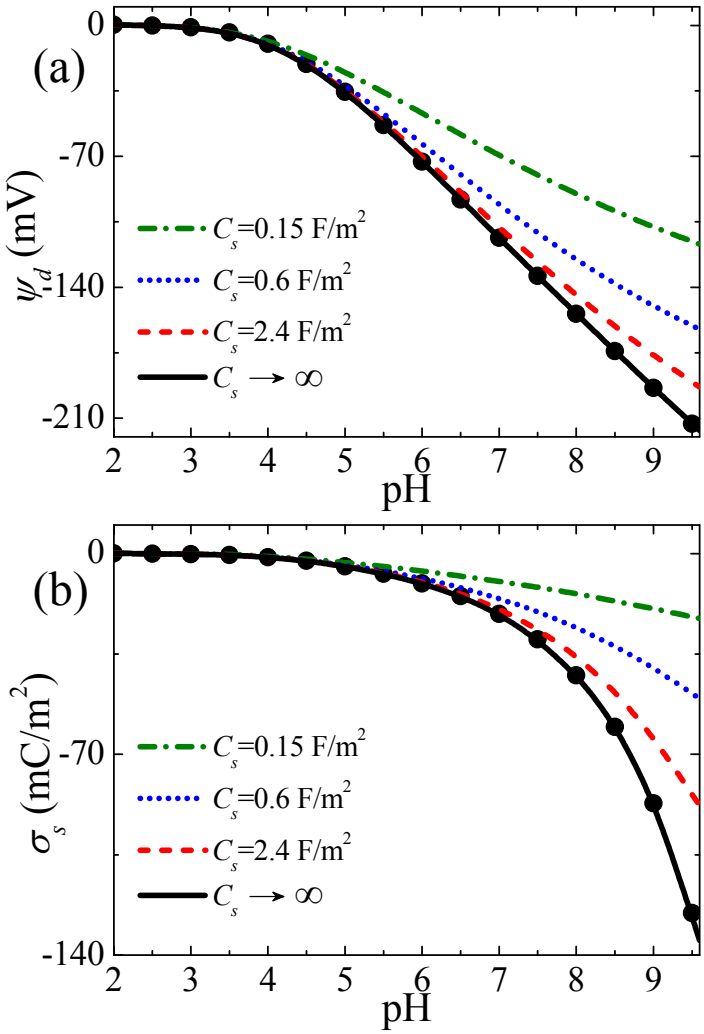

Fig. 3. Zeta potential ψ_d, (a), and surface charge density σ_s, (b), as a function of pH for various surface capacitance of the Stern layer C_s at the background salt concentration $C_{\mathrm{NaCl}} = 0.001$ M. Lines and spheres denote the numerical results with and without considering the Stern layer effect, respectively.

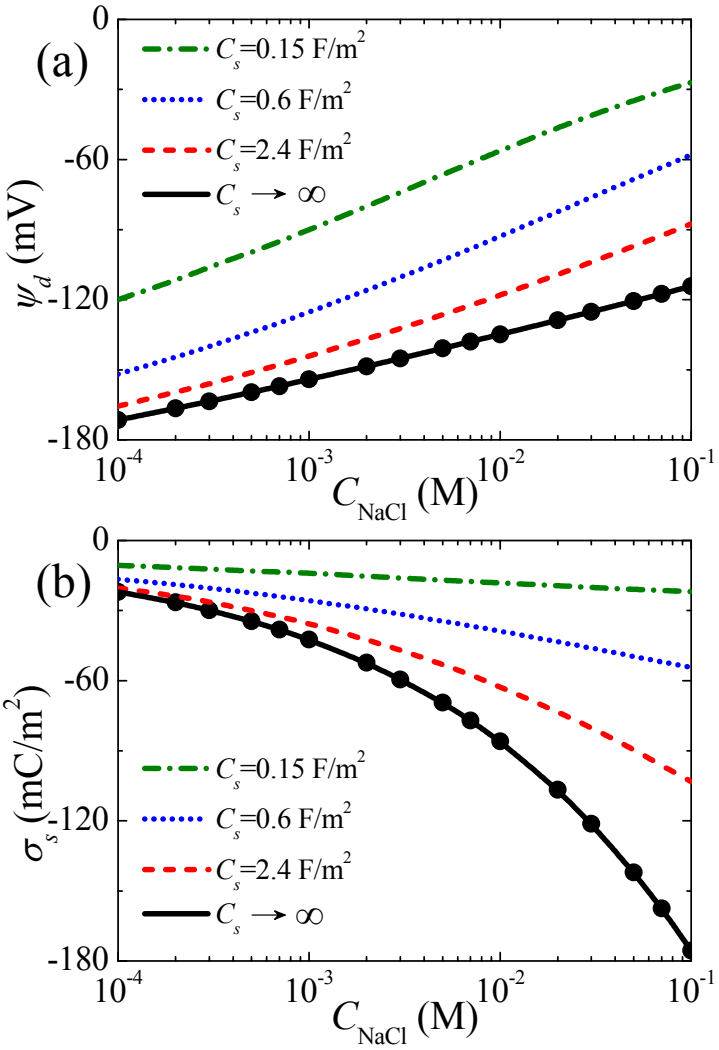

Fig. 4. Zeta potential ψ_d, (a), and surface charge density σ_s, (b), as a function of the background salt concentration C_{NaCl} for various surface capacitance of the Stern layer C_s at pH 8. Lines and spheres denote the numerical results with and without considering the Stern layer effect, respectively.

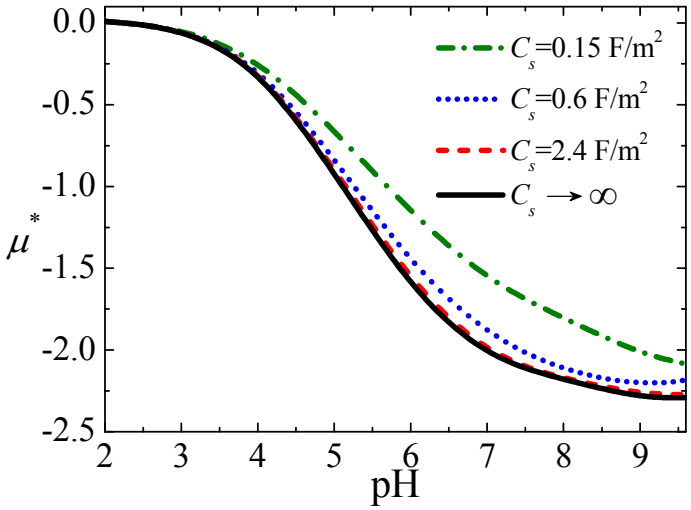

Fig. 5. Scaled electrophoretic mobility μ^* as a function of pH for various surface capacitance of the Stern layer C_s for the case of Fig. 3.

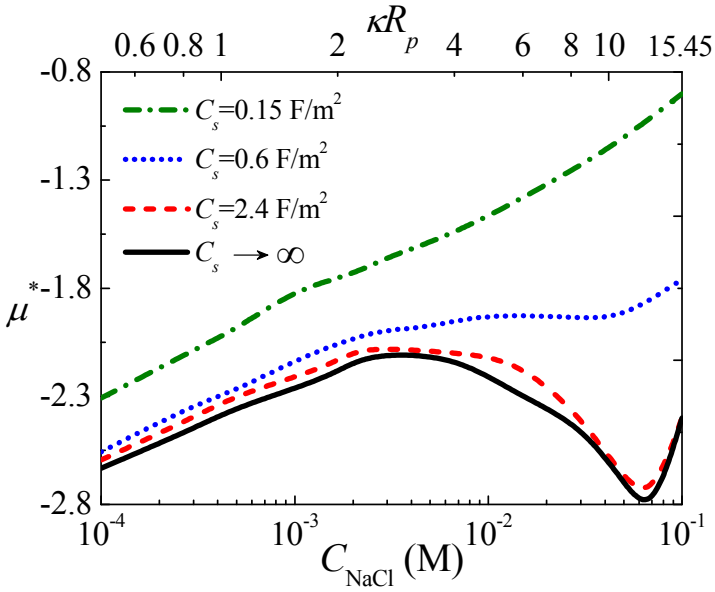

Fig. 6. Scaled electrophoretic mobility μ^* as a function of the background salt concentration C_{NaCl} (and the corresponding κR_p) for various surface capacitance of the Stern layer C_s for the case of Fig. 4.

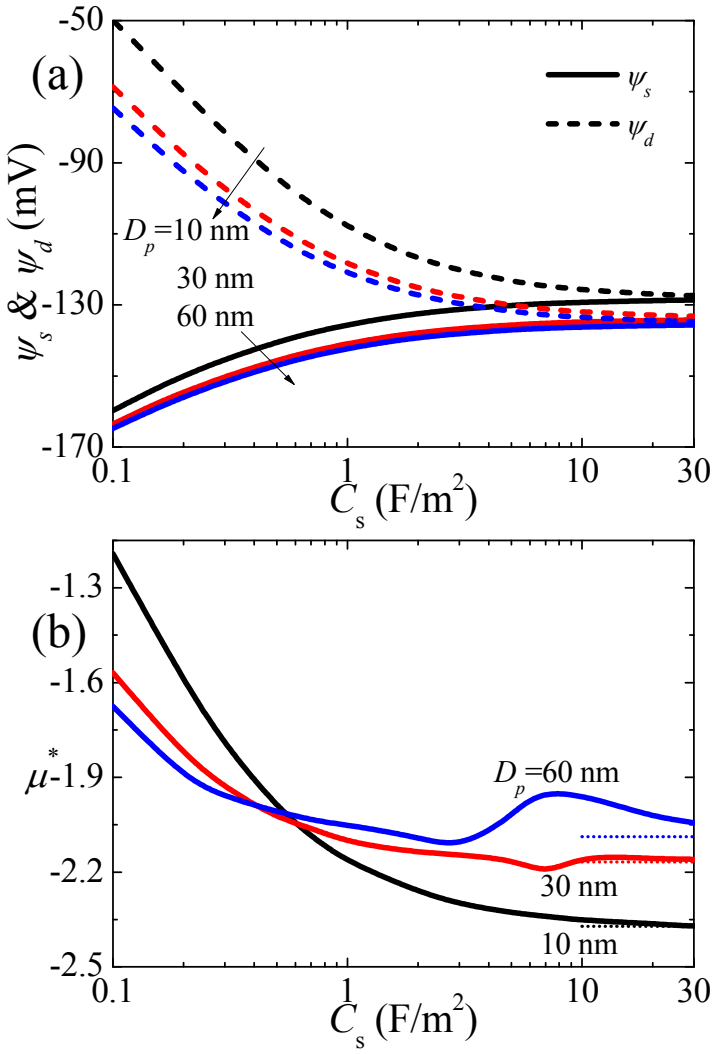

Fig. 7. Surface potential ψ_s (solid lines), zeta potential ψ_d (dashed lines), (a), and scaled electrophoretic mobility μ^*, (b), of a silica NP with various diameters D_p as a function of the surface capacitance of the Stern layer, C_s, at $C_{\mathrm{NaCl}} = 0.001$ M and pH 7.5. Dotted lines in (b) denote the results without considering the Stern layer effect.

TOC Graphic

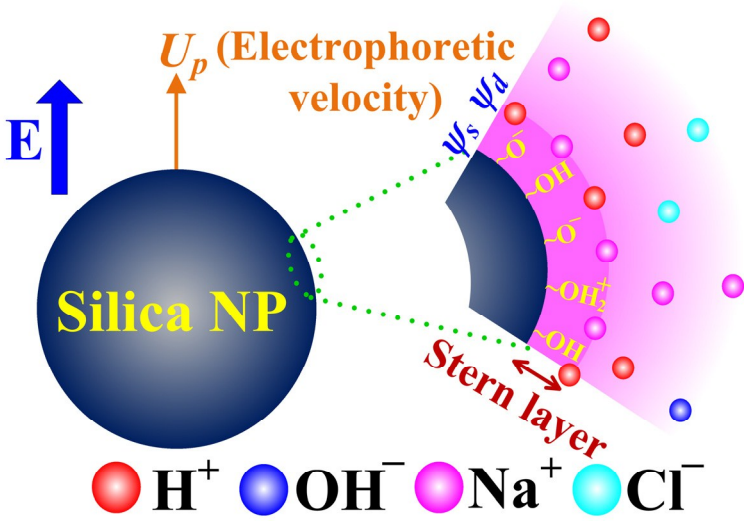

The Stern layer effect on the surface charge property and electrophoretic motion of pH-regulated silica nanoparticles is investigated theoretically.